Available online at www.sciencedirect.com
SCIENCE DIRECT®
Journal of Hydrology 278 (2003) 17–38
Journal of Hydrology
www.elsevier.com/locate/jhydrol

Evaluating the potential for measuring river discharge from space

David M. Bjerklie[a,*], S. Lawrence Dingman[a], Charles J. Vorosmarty[b], Carl H. Bolster[c], Russell G. Congalton[c]

[a]*Department of Earth Sciences, University of New Hampshire Durham, NH 03824, USA*
[b]*Institute for the Study of Earth, Oceans and Space, University of New Hampshire, Durham, NH, USA*
[c]*Department of Natural Resources, University of New Hampshire, Durham, NH, USA*

Received 29 May 2002; accepted 5 March 2003

Abstract

Numerous studies have demonstrated the potential usefulness of river hydraulic data obtained from satellites in developing general approaches to tracking floods and changes in river discharge from space. Few studies, however, have attempted to estimate the magnitude of discharge in rivers entirely from remotely obtained information. The present study uses multiple-regression analyses of hydraulic data from more than 1000 discharge measurements, ranging in magnitude from over 200,000 to less than 1 m^3/s, to develop multi-variate river discharge estimating equations that use various combinations of potentially observable variables to estimate river discharge. Uncertainty analysis indicates that existing satellite-based sensors can measure water-surface width (or surface area), water-surface elevation, and potentially the surface velocity of rivers with accuracies sufficient to provide estimates of discharge with average uncertainty of less than 20%. Development and validation of multi-variate rating equations that are applicable to the full range of rivers that can be observed from satellite sensors, development of techniques to accurately estimate the average depth in rivers from stage measurements, and development of techniques to accurately estimate the average velocity in rivers from surface-velocity measurements will be key to successful prediction of discharge from satellite observations.

Keywords: Estimation of river discharge; Satellite monitoring of rivers; River channel hydraulics; Multiple regression analysis of river hydraulic data; Multi-variate river discharge ratings

1. Introduction

Currently, less than 60% of the runoff from the continents is monitored at the point of inflow to the oceans (Fekete et al., 1999). The distribution of runoff within the continents is even less well monitored. Despite the importance of river discharge information, a comprehensive global river monitoring network faces numerous technological, economic, and institutional obstacles. As a result, gaging stations and access to river discharge information have been declining since the 1980s (Vorosmarty et al., 1999; IAHS, 2001). Hydrographic data obtained from satellites and other remote sources offer the possibility of broad and potentially frequent global coverage of river discharge estimates (Barrett, 1998). Thus, a method that uses remotely sensed data to estimate river discharge would provide a means to maintain or even increase the global streamflow monitoring

* Corresponding author.
E-mail address: bjerkliestemper@juno.com (D.M. Bjerklie).

0022-1694/03/$ - see front matter © 2003 Elsevier Science B.V. All rights reserved.
doi:10.1016/S0022-1694(03)00129-X

network and may, in the long run, be a cost-effective method to obtain needed river discharge data on a global scale.

The measurement of river discharge from space will fundamentally require a knowledge of the hydraulic relationship between river characteristics that can be observed from space-based platforms and river discharge. This paper reviews the types of river hydraulic information that can potentially be observed from space-based platforms and develops several general relationships that can use this information to estimate discharge. Hydraulic data from more than 1000 flow measurements in a wide range of rivers are used to develop and validate the relationships. An analysis of the impact of measurement error on prediction accuarcy is also undertaken. The approaches reviewed here are based on fundamental in-stream hydraulic relationships that are independent of watershed or basin predictor variables. Thus, the prediction methods are independent of regional and temporal climatic and physiographic variability and can be considered to be generally applicable to fluvial environments.

2. Estimating river discharge from hydraulic variables

For most rivers, discharge (Q) cannot be measured directly, but rather must be calculated from measurements of the pertinent hydraulic elements of the flow. Discharge at a river cross-section, from continuity, is the volumetric flow rate through that cross-section and is given by

$$Q = VWY = VA \tag{1}$$

where V is the average velocity, W is the water-surface width, Y the average water depth, and A the cross-sectional area perpendicular to the flow. Traditionally, Q is measured at selected cross-sections in a river by measurement of the velocity, depth and width at incremental vertical stations across the channel, and the incremental flow estimates are summed to obtain the discharge through the cross-section. These periodic velocity-area measurements of discharge are then correlated with measured water-surface elevation (stage) to develop a stage-discharge 'rating' for the cross-section. The stage-discharge rating equation takes the general form (Rantz et al., 1982; Herschey, 1998)

$$Q = a(Z - e)^m \tag{2}$$

where the coefficients a and m are characteristic of the specific channel cross-section, and e is the elevation of zero flow.

For the periods between measurements of Q, the stage (Z) is recorded and Q is inferred from the rating curve. Since the value of e represents the elevation of zero flow, the term $(Z - e)$ may be viewed as equivalent to the effective flow depth (Y) and thus the rating provides an estimate of discharge from the hydraulic flow depth. A rating equation such as Eq. (2) is developed for a particular river channel or cross-section, and would not be expected to be applicable to any other river location (Rantz et al., 1982). This is because change in stage (or depth) is used as an index to change in width and velocity, and is specific to the channel characteristics of the reach being measured. Thus, single variate discharge ratings cannot be generalized without a potential substantial loss in accuracy. Inclusion of additional hydraulic infromation into the rating model would improve the accuracy of the rating by accounting for more of the variability at any specific location.

Recently, Jasinski et al. (2001) used river stage obtained from satellite (TOPEX/Poseiden) altimetry data to develop discharge ratings for several locations in the Amazon basin by comparing the altimetry data with stage and discharge measured at existing gaging stations. The accuracy of the ratings varied depending on distance between the altimetry observation and the ground-measured discharge, and on the topography and the width of the river. This study demonstrated the feasibility of using satellite altimetry as a source of obtaining remote river stage information. However, ground-based discharge data were required to develop the rating, and the derived ratings could not be extrapolated to other rivers or reaches of the Amazon. While such a system might have advantages in some situations, it does not solve the problems imposed by the costs of establishing and periodically measuring discharge on-the-ground, and would not offer the prospect of expanding the global coverage of discharge observations. Thus, a general rating that can estimate discharge from remotely obtained hydraulic data without ground-based measurements

of discharge provides the best opportunity to capitaltize on satellite and other remote data sources.

A more general depth-discharge rating equation can be developed from the Manning equation which is widely viewed as generally applicable to natural rivers (Chow, 1959). Assuming a wide ($W > 10Y$) rectangular channel, the depth-discharge rating defined from the Manning equation is

$$Q = aY^{1.67} \tag{3}$$

with

$$a = WS^{0.5}/n. \tag{4}$$

In Eq. (3), the average depth is the dynamic predictive variable and the coefficient a can be directly calculated from channel properties and is comprised of a geometric component defined by W and a channel component defined by $S^{0.5}/n$ (which represents the balance between the gravitational energy supplied to the reach, S and the flow resistance, n). In a rectangular channel, W is constant and thus if S and n are constant, the coefficient a is constant. To the extent that S and n vary with depth, the exponent of Eq. (3) may also vary.

If a parabolic shape is assumed for the channel cross-section, a common assumption for natural channels (Chow, 1959), the width is related to the depth by $W^x = aY$ where x is the parabolic order. The derived depth-discharge rating from this assumption is

$$Q = aY^{(1/x+1.67)} \tag{5}$$

with

$$a = (W_m/Y_m^{1/x})(S^{0.5}/n) \tag{6}$$

The variable W_m is the maximum or bank-full width and Y_m the maximum or bank-full average depth.

A similar equation can also be developed that uses width as the rating variable:

$$Q = aW^{(1.67x+1)} \tag{7}$$

with

$$a = (Y_m^{1.67}/W_m^{1.67x})(S^{0.5}/n) \tag{8}$$

Eqs. (5) and (7) can be regarded as generally applicable discharge ratings for within-bank flow in the same sense that the Manning equation is generally applicable, under the assumption of a parabolic cross-section shape.

The channel resistance cannot be measured directly but is usually inferred from specific channel conditions including bed and bank material, channel irregularity (both in cross-section and planform shape) and other factors. In practice, the channel resistance is difficult to estimate with accuracy (Dingman and Sharma, 1997) and often varies considerably with discharge (Dingman, 1984). However, statistical studies by Riggs (1976), Jarrett (1984) and Dingman and Sharma (1997) have shown that reasonably accurate estimates of Q for within-bank flows can be obtained without resistance as an input variable, because the resistance varies with the channel geometry. Assuming that the hydraulic radius of the cross-section is equivalent to the mean depth (which would be expected for a wide channel), Dingman and Sharma (1997) show that for a wide range of rivers discharge can be estimated as:

$$Q = 4.62W^{1.17}Y^{1.57}S^{0.34} \tag{9}$$

with all variables in SI units. Eq. (9) was calibrated with over 500 flow measurements in 128 rivers and provides estimate accuracies, on average, in the range of 20% or better. This relationship can be considered a generally applicable multi-variate discharge rating because it includes the fundamental elements of uniform flow including the width, depth and slope. Additionally, since resistance is not an input variable, all of the necessary data can be measured either directly or remotely.

An equation similar to Eq. (9), which assumes that resistance is a function of the channel slope and geometry, can also be developed for situations where depth cannot be effectively measured, but velocity could be, such as in channels where there is substantial bed movement or bottom debris. The equation is developed from Eq. (1) with a general uniform flow equation such as Eq. (9), solving for the depth in terms of W, V and S, and then substituing this back into Eq. (1). Carrying through these operations yields an equation of the form:

$$Q = cW^bV^fS^g \tag{10}$$

In many situations it is difficult to establish the hydraulically meaningful channel slope that should be

used in a theoretically or statistically based equation. Davidian (1984) suggests that a hydraulically meaningful slope should be measured over a reach length on the order of 75 times the water depth. However, the water-surface slope in a channel reach may vary spatially and temporally due to unsteady and non-uniform flow conditions (Davidian, 1984), and because of this, the reach length and timing associated with the slope measurement can alter the 'true' uniform hydraulic slope associated with a particular discharge and channel geometry. Thus, consistent definitions of channel and water-surface slope will be important in attempting to apply equations involving those quantities. Given the potential difficulties of consistently measuring a water-surface slope that is hydraulically meaningful, a slope index may be used that considers the slope to be a constant rather than a variable. Such an index could be the topographic slope of the channel and thus might be related to channel morphology.

Alternatively, a relationship between discharge and an index velocity can be developed (Rantz et al., 1982) which eliminates the slope variable. Since the average velocity in a channel is proportional to the square root of slope and 2/3 power of the depth via the Manning equation, the mean velocity could be substituted for the depth and slope to obtain a width-velocity relationship that avoids the need to measure depth and slope but that still provides estimates over a wide range of flow conditions. The form of this equation would be

$$Q = cW^h V^i \tag{11}$$

where c is a coefficient, and the exponents h and i reflect the relationships between depth and both width and velocity.

3. Measurement of hydraulic variables from space

Few studies have attempted to estimate river discharge entirely from satellite and/or other remotely obtained information, although the potential has been pointed out (Koblinsky et al., 1993). Estimating the discharge in rivers via Eqs. (1), (5), (7), (9)–(11) requires a measure of the water-surface width, depth and water velocity, and/or river channel information including the water-surface slope, bank-full width and bank-full depth. The channel resistance is not a directly measurable quantity in the sense that it cannot be measured using an instrument, however it is related to the other geometric variables of the channel (Leopold et al., 1964; Bray, 1979; Dingman and Sharma, 1997) or can be evaluated by comparison with channel charcteristics where resistance values are known.

Satellite-based sensors and other remote data sources can be used to determine channel and water-surface width and water-surface area, water-surface elevation, channel slope and channel morphology (Table 1). In addition, there is a possibility that surface velocity can be measured at discrete locations across the river channel (Vorosmarty et al., 1999; Emmitt pers. commun., 2001). The key hydrographic variables that cannot be directly measured from satellite information or other remote data sources are average depth and average cross-sectional velocity. Thus, average depth and average cross-sectional velocity will need to be related, at least implicitly, to stage and surface velocity, respectively, if these variables are used for estimating discharge. Recently, Costa et al. (2000) have demonstrated that surface velocity measurements can effectively be used to estimate the mean velocity in a channel section.

Numerous studies have employed satellite-based imagery to estimate flood inundation area (Smith, 1997). However, few have used satellite derived data to track variability in river and flood stage elevations, and even fewer have attempted to quantitatively estimate river discharge. Landsat 7 multi-Spectral Scanner (MSS), Thematic Mapper (TM), and other visible/infrared spectrum sensors, and synthetic aperture radar (SAR) imagery from satellites have proven to be useful in tracking changes in water surface area (and widths) in floodplains and large rivers (Smith, 1997). Sippel et al. (1994) determined the inundation area of the Amazon River floodplain using a scanning multi-channel microwave radiometer (SMMR) mounted on the Nimbus 7 satellite. The SMMR sensor measures the microwave emission of the earth's surface, which can be correlated to ground saturation and open water at the surface; however

Table 1
Satellite and remote data sources

Data source	Hydrographic data type	Resolution	Relative Cost	Limitations/advantages	Coverage
Aerial photography	Surface features including width and channel shape. Stereoscopic pairs can also provide surface roughness and slope	High resolution depending on scale	Low	Limited by inability to see through cloud cover Can provide high resolution and detail and provides direct interpretation and yields from a range of spectral bands	Spatial—depends on scale. Temporal—Infrequent coverage
Visible spectrum digital imagery	Surface features including width, channel shape and coupled with a DEM surface roughness and slope	Depends on sensor, platform and orbital characteristics Aerial Imagery such as emerge (1) photography can be 1 m or less satellite based imagery such as Landsat 7 typically 10 m or less	Moderate to high depending on coverage (large areas are expensive)	Limited by inability to see through cloud cover Provides direct interpretation and yields information from a range of spectral bands	Spatial—can be large depending on desired resolution. Temporal—depends on orbital period and weather
Radar Imagery	Surface features including width, channel and roughness and used with interferometric methods can provide slope and possibly surface velocity using SAR with interferometry	Space based 10m to 30 m SAR surface velocity (not verified). Higher resolution with aerial	High	Interpretation may be difficult Can see through cloud cover and yields information from a range of spectral bands	Spatial—can be 150×150 km^2 or less depending on desired resolution. Temporal—depends on orbital period
Radar Altimetry	Elevation at discrete points which can be used to determine water surface heights (stage) and and possibly slope	Space based elevations typically 0.5 m but possible to 10 cm Higher resolution with aerial	High	Limited range of information Can see through cloud cover	Provides discrete point data with coverage that depends on the orbital period (frequency of repeat orbits)
Lidar	Surface velocity, water surface slope and stage	Possible to 10 cm/s for velocity (not verified) 5 cm elevation	Not evaluated	Limited by cloud cover and range of information is limited Interpretation of return may be simpler than radar	Provides discrete point data with coverage that depends on the orbital period (frequency of repeat orbits)
Topographic Maps and GIS	Static channel shape and slope and other static surface features	Depends on scale	Low	Temporally limited because it is a static data base Interpretation is direct	Spatial—depends on scale. Temporal—static
EPA Reach data base and other comparable data bases	Potentially reach lengths, channel types and other channel feaatures	Depends on data	Low	Temporally limited because it is a static data base Interpretation is direct	Dependent on available data

the resolution is low, on the order of 25 km, and the signal is attentuated by atmospheric moisture. Vorosmarty et al. (1996) correlated SMMR signals with discharge in the Amazon River, thus developing a discharge rating based on general moisture conditions within the basin. Brakenridge et al. (1994) used SAR images from ERS-1 to delineate flood inundation area coupled with topographic information to determine water-surface elevations during the 1993 Mississippi floods. Horritt (2000); Bates and DeRoo (2000) and Horritt et al. (2001) have used SAR imagery to delineate flood boundaries and calibrate river hydraulic models.

A method to estimate river discharge from aircraft has been developed (Kuprianov, 1978) that couples ground-based channel geometry information with surface velocity measurements made by photographing floats or other tracking substance introduced into the river by aerial drop. This method has a reported accuracy of 10% or better where winds are moderate (2– 3 m/s) and water-surface velocity is in the range of 1–2 m/s. Although this method relies on instruments introduced into the streamflow (the floats) to measure velocity, the measurement is made entirely from a remote platform (the aircraft).

Smith et al. (1996) estimated the discharge in three braided glacial rivers using reach-averaged water surface area obtained from RADARSAT SAR imagery. That study correlated the water-surface area in braided reaches (lengths on the order of 10 km) with discharge obtained from existing ground-based gaging stations to derive power function discharge ratings that use effective width (water-surface area divided by the reach length) as the predictor variable. The accuracy of the ratings varied in each river, ranging from 1.5% (for 11 estimated values) to 54% (19 estimated values). A single best-fit power function was also developed as a general rating for all of the rivers. Error associated with this function was much larger, providing accuracy only within a factor of 2 (100% error).

Smith et al. (1996) also pointed out that the total sinuosity was an important discriminator between the rivers studied. To test the predictive power of sinuosity, we used the data from Smith et al. (1996) to develop a general multi-parameter power function with reach averaged width as the dynamic variable and the average sinuosity as a channel constant to predict discharge in all the three braided rivers (data not shown). This relation reduced the standard error of the estimate by 30% and improved the slope of the regression compared to the width only relationship reported by Smith et al. (1996). These results suggest that morphologic features of a river channel that can be observed remotely and that are related to the energy dissipation process may be useful for remote discharge estimation. These features may include, in addition to channel sinuosity, meander wavelength, meander radius of curvature, bankfull width, width/depth ratio, and others (Leliavsky, 1966; Dury, 1976; Osterkamp et al., 1983; Rosgen, 1994).

In principle, it would seem that a width-discharge rating might be developed for a wide range of rivers, because width generally increases with increasing discharge. However, in nearly rectangular channels, or channels with highly irregular cross-sectional shape, width may change very little or in a highly non-linear way with discharge. This is shown in Fig. 1, which shows changes in width with discharge over a range of flows for the Mississippi River at Thebes, Illinois, and the Connecticut River at Thompsonville, Connecticut (USGS, 2001). The graphs demonstrate that in the Mississippi at Thebes width does indeed change linearly with discharge and could be used as an index to flow variation, whereas in the Connecticut at Thompsonville it changes non-linearly with very little change at higher discharges. Similarly, width changes very little with discharge in the Amazon River narrows at Obidos (Oltman, 1968). This condition may be common at many locations in larger rivers, and suggests that multi-variate discharge ratings that reflect general hydraulic relationships would be more universally applicable than relations based only on width. This also suggests that the best locations for evaluating river discharge from space, where width is the most readily observed hydraulic variable, are those channel reaches where width variation with dis-chage is most pronounced (Smith, 1997).

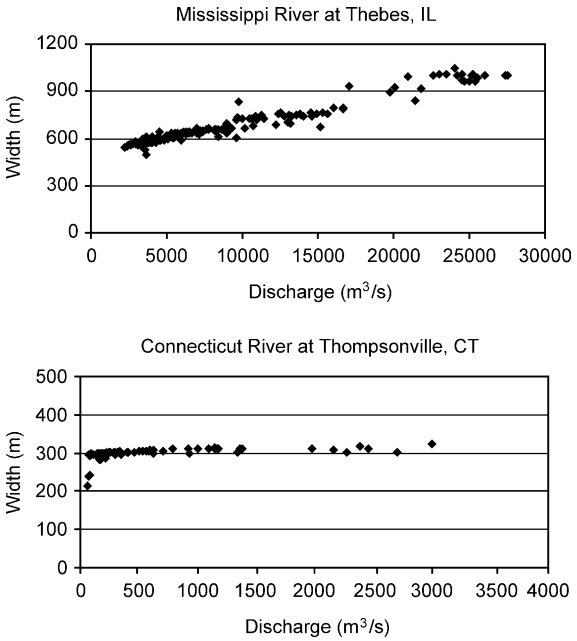

Fig. 1. Width versus discharge over a range of flows for the Mississippi River gage at Thebes, Illinois and the Connecticut River gage at Thompsonville, Connecticut (source of discharge measurements: US Geological Survey).

3.1. Measurement of width

Both channel width and water-surface width (and also the water-surface area) can be measured from a variety of sensors and imagers mounted on satellites and aircraft (Table 2), including panchromatic and infrared imagers, digital photography, and SAR (Barrett, 1998; University of Wisconsin Environmental Remote Sensing Center, 2001). The resolution of satellite mounted digital panchromatic sensors is within the same range as aircraft mounted sensors, indicating that satellite observation of width, because of the larger coverage, may be the preferred method to obtain this type of data. SAR is the only sensor that can measure the width in any atmospheric condition (Smith, 1997).

Panchromatic imagers have spatial resolution as high as 1 or 2 m and SAR imagers as high as 10 m (University of Wisconsin Environmental Remote Sensing Center, 2001). Additionally, the ability of a sensor to observe surface area or width change is not wholly a function of the resolution, such that relatively coarse resolution imagery may provide a measurement accuracy significantly better than the resolution may imply. Width estimates using any imager would be subject to errors associated with vegetation obscuring the water's edge and the bank and, in the case of SAR, wet ground, vegetation, wind roughening and rocks can also obscure the edge of water. With a combination of SAR imagery (to observe through cloud cover) and digital panchromatic imagery, it is conceivable that width could be observed with near global coverage on a repeat cycle of nearly one week.

3.2. Measurement of stage and depth

Radar altimetry has been successfully used to track water level elevations in large rivers, lakes and floodplains. Koblinsky et al. (1993) were able to use Geosat altimeter data to reproduce elevation changes at several locations in the Amazon River basin with an accuracy on the order of 0.7 m. The altimeter footprint ranges from 0.2 to 2 km, indicating that the target must be at least this wide to obtain a return unique to the water body. More recently, Birkett (1998) and Birkett et al. (2002) measured water surface elevation changes in several rivers around the globe (including rivers in the Amazon Basin, the Okavango River, the Indus River and the Congo River) using water surface elevation data obtained from the TOPEX/Posieden (T/P) altimeter and reported an accuracy ranging from 11 to 60 cm.

With the currently deployed T/P altimeter, the theoretical minimum river width that can be observed ranges from 0.58 to 1.16 km (Birkett et al., 2002) with accuracies ranging from 10 to 1 m. However, it is possible that the altimeter can obtain accurate water surface elevation measurements on rivers with widths as low as 50 m by altering the signal filtering algorithms (Rodriquez, pers. commun., 2001). The accuracy of the T/P altimeter (and altimeters in general) is strongly dependent on the surface conditions being observed (Birkett et al., 2002). Laser altimeters such as GLAS (NASA, 1997), which will be deployed on ICESAT, can track elevation changes to within 15 cm, and thus may provide significantly higher accuracies in river environments than possible with currently deployed radar altimeters.

Depth cannot be measured directly from remote data (Tables 1 and 2). Thus, this variable will need to be estimated, at least in part, from measurements

Table 2
Examples of river hydraulic variables observable from existing space based sensors

Observed variable	Satellite/sensor	Data type		Data and Resolution	Repeat observation frequency	Observational Issues
Water surface width and channel Morphology	TERRA/ASTER	Visible infrared		15 m	1–2 days	Cannot detect through clouds. Banks may be obscured by vegetation and shadows
		Thermal infrared Shortwave infrared				
	EROS A & B	Visible to infrared		1.5 m	Daily (with a constellation of satellites)	Cannot detect through clouds. Banks may be obscured by vegetation and shadows
	ERS2	SAR		12–26 m	6 days	Banks may be obscured by vegetation and wet soils
	SPOT 4	Panchromatic	visible	10 m	26 days	Cannot detect through clouds. Banks may be obscured by vegetation and shadows
	LANDSAT 7	Panchromatic	visible	15–60 m	16 days	Cannot detect through clouds. Banks may be obscured by vegetation and shadows
	IKONOS	Panchromatic	visible	1–4 m		Cannot detect through clouds. Banks may be obscured by vegetation and shadows
	RADARSAT	SAR		8–30 m	1–6 days	Banks may be obscured by vegetation and wet soils
Water surface stage and slope	ERS-2 TOPEX/ Posieden	Radar altimeter		10 cm	10 days	Repeat observations limited to large rivers using interferometry coupled with altimetry (unproven)
	RADARSAT	SAR		1 cm	1–6 days	
Water surface velocity		Lidar		NA		Signal obscured by surface wind and waves
		Radar		NA		Sensors have not been tested in rivers
		SAR		NA		

of stage coupled with other observable characteristics of the channel. Depth could be derived from repeated observations of stage over a wide range of flow conditions provided accurate topographic data or altimetric measurements of sufficient accuracy were available to determine the exposed bank elevation at each observed water level. However, in large rivers low flow depths may never be

observed, necessitating the estimation of the bankfull depth or other depth reference so that stage measurements can be converted to average water depths.

3.3. Measurement of water-surface slope

Water-surface slopes on the Amazon River and some of its larger tributaries have been estimated by Mertes et al. (1996) and Dunne et al. (1998) using SEASAT and Birkett et al. (2001) using T/P.

All of these estimates have been made from sea-level (the mouth of the Amazon) to an inland point hundreds or thousands of kilometers upstream. The long reaches that were evaluated minimized the impact of altimeter accuracy on the estimates. Birkett et al. (2002) were also able to observe temporal changes in water surface slope in the mainstem of the Amazon over long reaches.

In the Amazon River at Obidos, the water depth is on the order of 40–50 m and hydraulically meaningful water-surface gradients are on the order of 1 cm/km (Oltman, 1968). Thus, given an optimistic altimeter error of 10–20 cm, a reach of 5–10 km could conceivably result in slope estimates ranging from negative values to 8 times the actual value. This suggests that slope information obtained from the current generation of altimeters would not provide sufficient spatial resolution to be hydraulically meaningful. Averaging the slope obtained from a large sampling of water slope measurements may be the most meaningful slope information that can be considered reliable.

One approach to obtaining more accurate water surface slope measurements could be through the use of interferometric SAR. With this technique, water-surface elevation changes on the order of 1 cm can be detected in large rivers and flooded areas (Alsdorf et al. 2000, 2001) and, when coupled with high resolution topographic information, could be used to estimate water-surface slopes across a flooded area as well as within a river. Laser altimeters may also provide a means to accurately measure hydraulically meaningful water-surface slopes because the altimeter could simultaneously measure the elevation at two points in a channel reach.

3.4. Measurement of water-surface velocity

Surface velocity in rivers is potentially measurable from satellites with doppler lidar or radar. However, surface winds and waves on the water body could significantly interfere with the measurement (Vorosmarty et al., 1999) although observing limitations have not been fully evaluated. Theoretical (e.g. the Prandtl-von Karman velocity profile) or empirical relations would be required to translate surface velocity to average velocity; however, surface velocity could potentially provide an index of average flow velocity and hence be directly useful in predicting discharge. Based on information supplied by Emmitt pers. commun. (2001), a satellite mounted doppler lidar sensor that could observe surface velocity would have a footprint of approximately 10 m with 75 m between observations along a track, and have a measurement accuracy on the order of 0.1 m/s. Given these specifications, the lidar could observe two to three surface velocity 'points' across a 200 m wide river reach. There is no guarantee that the satellite track would cross the river reach perpendicular to the flow, thus the point measurements may be skewed across the channel. This should not be a problem provided the distance to each bank can be evaluated from another source (e.g. a concurrent image of the channel and knowledge of the satellite track). Despite the potential limitations, if surface velocity were measured and can be used to infer average velocity, there is the potential for measuring all elements of Eq. (1) simultaneously and thus enabling direct calculation of discharge.

3.5. Observation of channel morphology

Valley and channel features such as the channel sinuosity, channel slope, meander length, and meander radius of curvature can be observed from a variety of data sources including visible and infrared spectrum images, SAR images, DEMs and topographic map information. Since these features are considered relatively stable over short time frames, the frequency and timing of observations is not a limiting factor, and therefore high resolution panchromatic images could be used to measure them when weather conditions permit.

4. Estimating river discharge

Based on the above discussion, there is a possibility that the hydraulic elements of Eq. (1) can all be measured simultaneously from satellites. If so, discharge could be calculated directly, with an accuracy dependent on the accuracy and precision of the individual measurements of water-surface width, surface velocity, and stage and of the estimations of mean velocity and mean depth from observations of surface velocity and stage. Because there is a potential that stage or surface velocity will not be observed with confidence (e.g. under strong winds or where topography obscures the signal) there will be many situations when all three of the key variables cannot be observed at the same time. In these situations statistically based relationships such as described by Eqs. (9)–(11), may be useful.

4.1. Statistically based estimation methods

To explore the predictive characteristics of different combinations of potentially observable (or estimated) river hydraulic variables, a set of generally applicable river discharge estimation equations (models) were developed based on Eqs. (5), (7), (9)–(11). The models were derived using multiple regression analysis of hydraulic data from 1012 discharge measurements in 102 rivers in the United States and New Zealand, including four measurements from the Amazon River at Obidos. The data base includes a wide range of river conditions (Table 3) and was randomly divided into a calibration data set and a validation data set each containing 506 measurements. The four Amazon River measurements were equally divided between the calibration and validation data sets.

The data base includes 569 discharge measurements with reach averaged (generally three or more cross-sections representing a reach length 5 or more times the width) values of water-surface width, average water-surface depth, average velocity, and water-surface slope measured concurrently with the discharge. These data were obtained from Barnes (1967), Hicks and Mason (1991) and Coon (1998). Because these data are reach-averaged, the hydraulic geometry and velocity values are representative of the energy and resistance relationships within the channel, and less a reflection of conditions at a single cross-section. In addition, the reported width approximates the water-surface area divided by the reach length, consistent with Smith et al. (1996). In this way, the data are consistent with what might be obtained from remote imagery capable of providing reach averaged width, channel slope, and surface velocity.

The reach-averaged data include only two discharge measurements greater than 10,000 m^3/s. In order to include more large flows in the data base, 443 additional measurements representative of the larger rivers of North America were obtained from USGS, (2001) and data from four measurements for

Table 3
Range of hydraulic parameters in calibration and validation data sets

Parameter	Symbol	Units	Mean	Standard deviation	Coefficient of variance	Maximum	Minimum
Calibration data N = 506							
Discharge	*Q*	m^3/s	1585	12,260	7.74	216,000	0.01
Top width	*W*	m	146	206	1.41	2290	2.90
Average depth (hydraulic radius)	*Y*	m	2.48	3.56	1.44	48.03	0.18
Average velocity	*V*	m/s	1.12	0.66	0.59	5.10	0.02
Water surface slope (average)	*S*	m/m	0.00278	0.00572	2.06	0.04	0.0000007
Valdiation data N = 506							
Discharge	*Q*	m^3/s	1666	13,184	7.91	283,170	0.05
Top width	*W*	m	158	211	1.34	2300	5.40
Average depth (hydraulic radius)	*Y*	m	2.73	3.53	1.29	50.33	0.14
Average velocity	*V*	m/s	1.13	0.61	0.54	3.61	0.07
Water surface slope (average)	*S*	m/m	0.00243	0.00474	1.95	0.04	0.0000007

the Amazon River at Obidos, Brazil were also included (Oltman, 1968; Dury, 1976). These large river discharge measurements are not reach averaged, and therefore have a certain incompatibility with the rest of the data in the data base. However, it is anticipated that hydraulic variability between the measurement section and the reach as a whole is not large, and that the number of observations will average out the variability. In addtion, inspection of the channel characteristics at the measurement sections for these rivers do not indicate any channel constraints from bridges or other structures.

The discharge data are all in-bank and do not represent overbank flow conditions. In general, the data were obtained from relatively straight single thread channel sections, and therefore do not necessarily reflect the hydraulic conditions in more complex or less constrained channel patterns. Because of this, the derived regression coefficients may be biased towards these types of channels, reflecting typical relationships between width and depth, depth and resistance, and velocity and depth that would be found in straight channels. However, because the models are based on, and include, the fundamental hydraulic variables of uniform flow, the resultant regression equations are considered to remain generally representative of uniform flow relationships for any defined channel.

Similar to Dingman and Sharma (1997), the predictive models were assumed to be multiplicative. The form of the prediction equations (models) that were developed are based on Eqs. (5) (7), (9)–(11), as follows:

Model 1 (Eq. (9))

$$Q = c_1 W^a Y^b S^d \tag{12}$$

Model 2 (Eq. (11))

$$Q = c_2 W^e V^f S^g \tag{13}$$

Model 3 (Eq. (10))

$$Q = c_3 W^e V^f \tag{14}$$

Model 4 (Eq. (5))

$$Q = c_4 W_m^g Y_m^h S^i Y^j \tag{15}$$

Model 5 (Eq. (7))

$$Q = c_5 W_m^k Y_m^l S^m W^n \tag{16}$$

Models 1, 2, 4 and 5 use the water-surface slope as a prediction variable. However, the USGS discharge measurement data base does not include slope as a measured parameter. Therefore, a channel slope for these river stations was measured manually from 1:24,000 scale USGS topographic maps over one contour interval. This results in a constant slope value for all of the flow measurements at a particular river station, implying slope as a geomorphic characteristic of the river.

The implication of using a constant slope is explored by comparing two realizations of Model 1 developed from the reach averaged data base, that includes a unique measured slope for all discharge measurements (minimum of five) at each river station (excluding the Barnes (1967) data, which includes only one flow measurement at each station). The first model uses slope as a dynamic variable and the second uses a slope obtained by averaging all of the measured slopes over the entire discharge range at each river station. The comparison shows nearly identical regression models (Table 4). Based on this comparison, we conclude that using an average slope, or a channel slope obtained from topographic information that is a constant for a river reach, can be used in lieu of a measured slope, thus obviating the need to track water surface slope as a dynamic prediction variable. These results indicate also that the USGS flow measurement data, which includes width, average depth, average velocity, and discharge (but not slope) can be combined with the reach averaged data base (which includes a measured slope) using a slope measured from 1:24,000 scale USGS topographic maps for each station. In the remainder of this paper, all of the regression models and all discussion of slope as a prediction variable assume a constant slope for each river station, developed either as an average of many measured values, or obtained from topography.

Using the entire calibration data set ($N = 506$), the following regression models are developed:

Model 1:

$$Q = 7.22 W^{1.02} Y^{1.74} S^{0.35} \tag{17}$$

Model 2:

$$Q = 0.09 W^{1.21} V^{1.53} S^{-0.30} \tag{18}$$

Table 4
Comparison of regression models using constant and variable slope

Model	*Regression statistics*												
	N	R^2	Standard error regression		Relative residual $(Q^*-Q)/Q$	Log residual $(\log Q^*-\log Q)$	Actual Residual (Q^*-Q)	Coefficients	Value	Standard error	Upper 95%	Lower 95%	p
Variable Slope $Q=4.57W^{1.18}Y^{1.74}S^{0.35}$	545	0.95	0.19	Mean	0.12	0.001	14.6	Intercept	4.57	1.14	5.97	3.50	<0.0001
				Standard deviation	0.69	0.189	113.8	W	1.18	0.03	1.24	1.12	<0.0001
								Y	1.74	0.04	1.82	1.67	<0.0001
								S	0.35	0.02	0.38	0.32	<0.0001
Constant slope $Q=4.60W^{1.17}Y^{1.76}S^{0.35}$	545	0.95	0.20	Mean	0.14	−0.001	11.4	Intercept	4.60	1.16	6.21	3.42	<0.0001
				Standard deviation	0.87	0.202	113.0	W	1.17	0.03	1.23	1.10	<0.0001
								Y	1.78	0.04	1.86	1.69	<0.0001
								S	0.35	0.02	0.39	0.31	<0.0001

Model 3:

$$Q = 0.23W^{1.46}V^{1.39} \tag{19}$$

Model 4:

$$Q = 3.55W_{\mathrm{m}}^{1.19}Y_{\mathrm{m}}^{-0.84}S^{0.3}Y^{2.17} \tag{20}$$

Model 5:

$$Q = 1.07W_{\mathrm{m}}^{-1.61}Y_{\mathrm{m}}^{1.11}S^{0.08}W^{2.65} \tag{21}$$

The values for Y_{m} and W_{m} used in the regresssion analysis are obtained as the maximum value for all of the flow measurements at each river station, and thus are constant for each station. The possiblity that the Amazon River measurements skewed the regression results was evaluated by removing them from the calibration data set and re-running the regression analysis. It was found that the Amazon data did not significantly impact the regression results.

The four regression models varied in their ability to describe the observed data. Comparative statistics between the models are shown on Table 5 and indicate that Models 1, 2 and 3 perform comparably well, and that Model 4 does not perform as well as Models 1, 2 and 3 but is better than Model 5. The intercept and coefficient of the slope for Model 5 are not significantly different than zero at the 95% confidence level. Since the form of the model is based on the Manning equation, slope would be expected to be a significant predictor variable as it is in Model 1. The reason for this outcome may be due to the fact that width by itself is not an especially good predictor variable at many specific river stations (as indicated in Fig. 1), and thus a constant slope at each river station does not contribute to explaining at-a-station variation. The standard error of the estimate (standard deviation of the log residuals) for Model 5 is nearly twice as large as the standard errors for Model 1, 2 and 3, and indicates that 67% of the predictions using this model fall within a wide margin (factor of 2.75). Because of the relatively poor performance of Model 5 it is not evaluated further.

For comparative purposes, Table 5 also lists regression results for three single-variate models that use each element of Eq. (1) (W, Y and V) to predict Q. These models indicate that depth, by itself, predicts discharge better than width and has a lower standard error than Model 5, and would be expected to

Table 5
Regression model comparison

Model	*Regression statistics*								
Model	R^2	Standard error regression	Coefficients	Value	Standard error	Upper 95%	Lower 95%	*t* stat	*p*
Model 1									
$\log Q = 0.86 + 1.02 \log W + 1.74 \log Y + 0.35 \log S$	0.95	0.23	Intercept	0.86	0.06	0.98	0.73	13.40	<0.0001
$(Q = 7.22W^{1.02}Y^{1.74}S^{0.35})$			W	1.02	0.03	1.07	0.96	35.16	<0.0001
			Y	1.74	0.04	1.82	1.66	42.07	<0.0001
			S	0.35	0.02	0.40	0.31	15.27	<0.0001
Model 2									
$\log Q = -1.06 + 1.21 \log W + 1.53 \log V - 0.30 \log S$	0.97	0.19	Intercept	−1.06	0.04	−0.98	−1.14	−26.22	<0.0001
$(Q = 0.09W^{1.21}V^{1.53}S^{-0.30})$			W	1.21	0.02	1.25	1.16	53.65	<0.0001
			V	1.53	0.03	1.59	1.47	51.85	<0.0001
			S	−0.30	0.02	−0.26	−0.33	−15.29	<0.0001
Model 3									
$\log Q = -0.63 + 1.46 \log W + 1.39 \log V$	0.95	0.23	Intercept	−0.63	0.04	−0.56	−0.70	−17.93	<0.0001
$(Q = 0.23W^{1.46}V^{1.39})$			W	1.46	0.03	1.45	1.32	40.98	<0.0001
			V	1.39	0.02	1.50	1.43	80.57	<0.0001
Model 4									
$\log Q = 0.55 + 1.19 \log W_m - 0.84 \log Y_m + 0.3 \log S + 2.17 \log Y$	0.93	0.28	Intercept	0.55	0.11	0.76	0.34	5.19	<0.0001
$(Q = 3.55W_m^{1.19}Y_m^{-0.84}S^{0.30}Y^{2.17})$			W_m	1.19	0.06	1.29	1.08	21.42	<0.0001
			Y_m	−0.84	0.11	−0.63	−1.06	−7.64	<0.0001
			S	0.30	0.03	0.37	0.24	9.48	<0.0001
			Y	2.17	0.05	2.27	2.06	42.11	<0.0001
Model 5									
$\log Q = 0.03 - 1.61 \log W_m + 1.11 \log Y_m + 0.08 \log S + 2.65 \log Y$	0.83	0.44	Intercept	0.03	0.17	0.36	−0.30	0.17	0.86
$(Q = 1.07W_m^{-1.61}Y_m^{1.11}S^{0.08}W^{2.65})$			W_m	−1.61	0.16	−1.30	−1.92	−10.24	<0.0001
			Y_m	1.11	0.16	1.42	0.79	6.86	<0.0001
			S	0.08	0.05	0.18	−0.02	1.53	0.13
			W	2.65	0.13	2.90	2.39	20.00	<0.0001
Comparative single-variate Models									
$Q - W$									
$\log Q = -0.98 + 1.62 \log W$	0.79	0.49	Intercept	−0.97	0.07	−0.84	−1.11	−13.74	<0.0001
$(Q = 0.11W^{1.62})$			W	1.62	0.04	1.69	1.55	43.85	<0.0001
$Q - Y$									
$\log Q = 1.49 + 2.46 \log Y$	0.84	0.43	Intercept	1.49	0.02	1.54	1.45	70.33	<0.0001
$(Q = 30.90Y^{2.46})$			Y	2.46	0.05	2.55	2.37	51.64	<0.0001
$Q - V$									
$\log Q = 2.07 + 1.96 \log V$	0.33	0.87	Intercept	2.07	0.04	2.15	2.00	52.92	<0.0001
$(Q = 117.49V^{1.96})$			V	1.95	0.12	2.20	1.72	15.90	<0.0001

predict discharge to within a factor of 2.7, 67% of the time (the standard error is the standard deviation of the log residual, and its antilog represents the standard deviation of the fractional errors between the predicted and observed values). Width by itself would be expected to predict discharge within a factor of 3, 67% of the time. Velocity would predict discharge within a factor of 7.4, 67% of the time, indicating that by itself it is a very poor predictor of discharge.

The validation statistics for Models 1, 2, 3 and 4 and the Dingman and Sharma Model (Eq. (9)) are compared in Table 6. Comparative statistics include the mean and standard deviation of the following quantities:

$$\text{Relative residual} = (Q^* - Q)/Q \quad (22)$$

$$\text{Log residual} = \log(Q^*) - \log(Q) \quad (23)$$

$$\text{Actual residual} = Q^* - Q \quad (24)$$

In addition, the number of predictions within a specified percent error interval (percent different than the observed) are also tabulated for 20, 50 and 100% error. Fig. 2 shows the predicted discharge (Q^*) plotted against the observed discharge (Q) for each model, along with an upper and lower envelope curve defined by the ±50% error in the observed value.

The log and actual residuals indicate that Model 1 and the Dingman and Sharma model tend to over-predict discharge and Models 2, 3 and 4 tend to under-predict discharge (Table 6 and Fig. 2). Model 1 shows the least overall prediction bias, and the Dingman and Sharma model has the highest. The mean relative error indicates the average percent error of the predictions. Model 2 performs the best in this regard, with an average relative error of 10%. Average relative error for Model 1, 3 and 4 are less than 20%. The antilog of the mean of the log residuals indicates the fractional error between the predicted and observed discharge (i.e. the ratio Q^*/Q), which can be regarded as a correction factor. This measure of error shows that Model 1 has the highest mean accuracy (with a ratio of less than 1%), and that Models 2, 3 and 4 all show mean accuracy within 5%.

Table 6
Regression model validation statistics

Model	Validation statistics						
		Relative residual $(Q^* - Q)/Q$	Log residual $(\log Q^* - \log Q)$	Actual residual $(Q^* - Q)$	Percent of predictions within 20, 50 and 100% of the observed		
					20%	50%	100%
Model 1							
$Q = 7.22W^{1.02}Y^{1.74}S^{0.35}$	Mean	0.16	0.004	243	39%	82%	90%
	Standard deviation	0.81	0.207	5059			
Model 2							
$Q = 0.09W^{1.21}V^{1.53}S^{-0.3}$	Mean	0.07	−0.017	−615	37%	79%	94%
	Standard deviation	0.58	0.195	7129			
Model 3							
$Q = 0.23W^{1.46}V^{1.39}$	Mean	0.10	−0.024	−790	32%	71%	93%
	Standard deviation	0.71	0.231	9946			
Model 4							
$Q = 3.55W_m^{1.19}Y_m^{-0.84}S^{0.30}Y^{2.17}$	Mean	0.17	−0.016	−119	28%	73%	89%
	Standard deviation	0.99	0.243	5333			
Dingman and Sharma Model							
$Q = 4.62W^{1.17}Y^{1.57}S^{0.34}$	Mean	0.43	0.092	763	41%	74%	86%
	Standard deviation	1.01	0.215	7644			

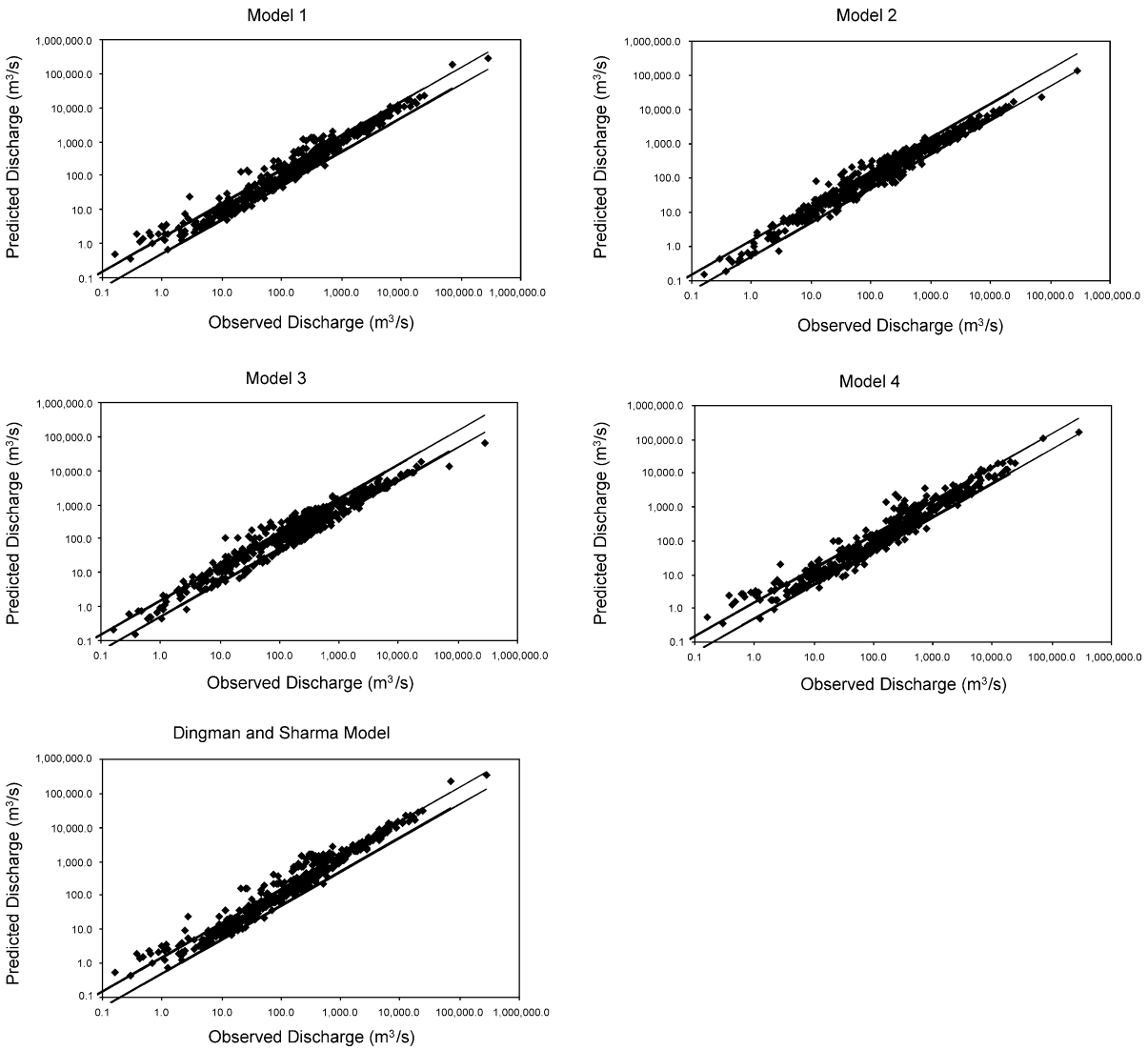

Fig. 2. Predicted discharge (Q^*) plotted against observed discharge (Q) for the validation data set using Models 1, 2, 3, 4 and the Dingman and Sharma Model. ±50% of the observed discharge is shown as envelope curves through the plotted data.

Model 2 shows the least overall prediction error variability, as indicated by the standard deviation of the relative error and the log residual. The error percentiles indicate that Models 1, 2 and the Dingman and Sharma model are comparable.

Inspection of Fig. 2 indicates that the predictive characteristics of the models vary for different ranges of discharge. These differences are evaluated by comparing the distribution of the relative residual with observed discharge. To facilitate comparison, the mean and standard deviation of the relative residuals have been averaged within four categories of discharge range (0–10, 10–100, 100–1000 and >1000 m^3/s). Models 1, 4 and the Dingman Sharma model tend to over-predict primarily in the low discharge range (0–10 m^3/s). This suggests that these models will have the best results in medium to large rivers where discharge typically ranges above 10 m^3/s. The reason for this may be that the relationship between resistance and the channel

geometry cannot be fully represented by a single regression intercept (model coefficient). Models 2 and 3 also tends to over-predict discharge in the low range (0–10 and 10–100 m^3/s) but also under-predicts in the high discharge range ($>1000\ m^3/s$). This result indicates that Models 2 and 3 would do better if the coefficients varied with discharge, i.e. different model coefficients were calculated for different flow ranges. The Dingman and Sharma Model shows a consistent over-prediction for all flow ranges, which may result because it was developed from a data set with fewer large rivers (also suggesting that statistical models such as these would be improved if they were developed for specific flow ranges).

Prediction variability, as indicated by the upper and lower standard deviation of the relative residuals, is reduced in the highest discharge range for Models 1, 2, 3 and 4 (Fig. 3). This indicates that model precision is improved for the larger rivers. The Dingman and Sharma model does not follow this trend, which again may be due to the presence of fewer large rivers in the data base used to develop it. The validation statistics indicate that prediction models based on Models 1, 2, 3 and 4 could all be used as general discharge estimating models, with mean accuracy of less than 20% in all cases. The variability of the estimates would be expected to be within ±50% of the acutal value on the order of 2/3 of the time. The prediction accuracy would be improved for medium and large rivers.

As a comparison, under good measurement conditions, the accuracy of a discharge measurement made on the ground with standard techniques is assumed to be in the range of 2 to 4% of the actual value at least 2/3 of the time (Rantz et al., 1982; Herschey, 1998). The accuracy of measurements made using the slope-area method (usually for large discharges that could not be meausred using standard techniques), which is based on after-the-fact measurements of the flow width, depth, energy slope and flow resistance using the Manning or comparable uniform flow equation, are not explicitly known because it depends on field judgement and the quality of the measured data (Kirby, 1987). However it is often reported that good measurements have an accuracy between 10 and 20% (Herschey, 1998).

The development of the rating curve averages out some of the error associated with the discharge measurements, however interpolation from the rating curve may also introduce error, especially if the rating curve is subject to change over time. The accuracy of estimates made from the rating curve diminishes with extrapolation beyond the highest and lowest measured discharges because the nature of the 'true' rating beyond the measured values is not known. Additionally, hysteresis effects may not be adequately reflected in the rating. Dickerson (1967) suggests that estimating future (uncalibrated) discharge values from a rating curve may range from +13 to −11% at the 80% confidence level, and from +21 to −17% at the 95% confidence level.

4.2. Measurement uncertainty analysis

Models 1, 2, 3 and 4, and Eq. (1) enable exploration of the impact that potential uncertainty (error) in measurement of the dynamic variables W, Y and V would have on the accuracy of discharge predictions. To do this, (the measured variables were assumed to be error free which is not really the case), typical measurement accuracies were assigned to each variable, and then varied randomly assuming a normal distribution such that the mean measurement uncertainty for the entire data base is zero and 95% of the uncertainties are within the assigned accuracy. The modified data were then used to re-estimate the discharge in the validation data base and then these values were compared via the relative residual to the estimates that assumed no uncertainty. A maximum and minimum measurement accuracy is assumed for each dynamic variable. For W, the minimum assumed measurement uncertainty is 1 m and the maximum is 10 m, which would be consistent with many of the current SAR and visible spectrum sensors (Table 2). The minimum assumed measurement uncertainity in water-surface elevation (as a proxy for Y) is 0.1 m and the maximum is 0.5 m, consistent with the range associated with current satellite altimeters (Birkett, 1998; Birkett et al., 2002). The minimum measurement uncertainty in V is assumed to be 0.1 m/s, which is the low end of the anticipated accuracy of a surface velocity measurement (Emmitt pers. commun., 2001), and the maximum was arbitrarily chosen to be 0.5 m/s (since the measurement of surface velocity from satellites has not been tested).

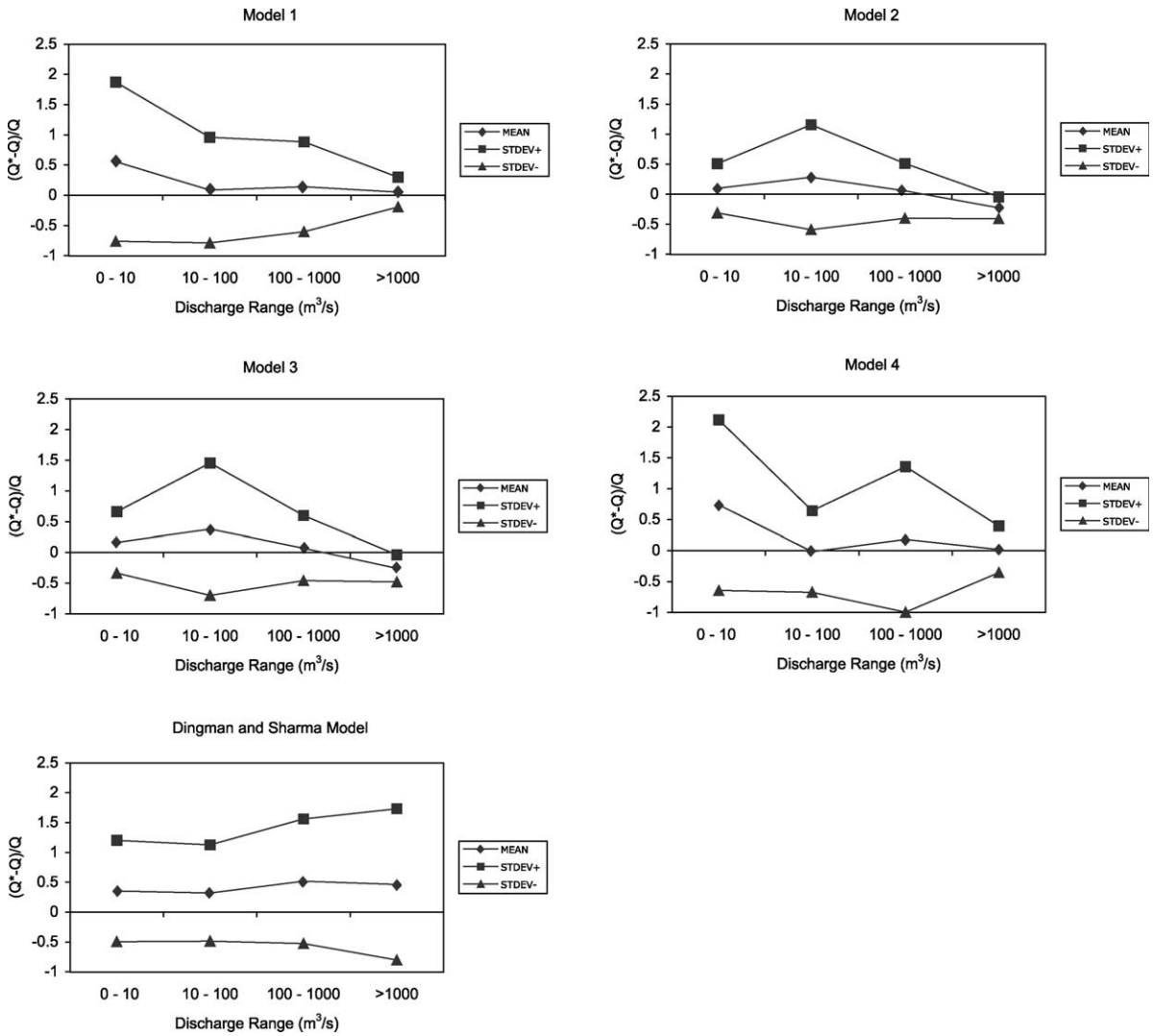

Fig. 3. Variation of the mean and standard deviation of the relative residuals averaged within ranges of observed discharge. The upper and lower lines are plus and minus one standard deviation from the mean. Multiplying the relative residual by 100 gives the percent error. The number of observations in each range, from lowest to highest range, are 71, 132, 209 and 94 respectively.

This analysis does not consider the potential uncertainity in estimating channel slope or the other characteristic channel values W_m and Y_m. These variables could be determined by a number of methods, including (1) estimation from topographic mapping and geomorphologic considerations, (2) measurement from repeated satellite observations, and (3) measurement via field surveys. The magnitude of uncertainty associated with determining the channel characteristics will depend in large part on the accuracy of available topographic information and availability of channel survey data. The analysis also does not consider the uncertainity associated with estimating the average velocity from the surface velocity measurements or the uncertainty associated with converting stage to average depth. However, Costa et al. (2000) has shown that the surface velocity can be used to estimate the mean velocity in a cross-section with good overall results by using a simple correction factor of 0.85 (Rantz et al., 1982).

The assumed measurement uncertainties are distributed with a mean of zero. For this reason, the standard deviation of the relative residuals is used as the indicator of the impact of measurement uncertainty on the predictions. The standard deviation of the relative residuals as a function of discharge category for the maximum assumed uncertainty (error), the minimum assumed uncertainty, and the case with no uncertainity is shown on Fig. 4. The least variability is associated with using Eq. (1) because there is no associated statistical error. All of the plots in Fig. 4 show that the impact of maximum measurement uncertainty on prediction variability, relative to the no uncertainity case, becomes pronounced below a discharge of 10 m^3/s. The impact of maximum uncertainty for discharge above 10 m^3/s is greatest for Eq. (1) and Models 2 and 3. This result shows the effect of compounding errors in the case of

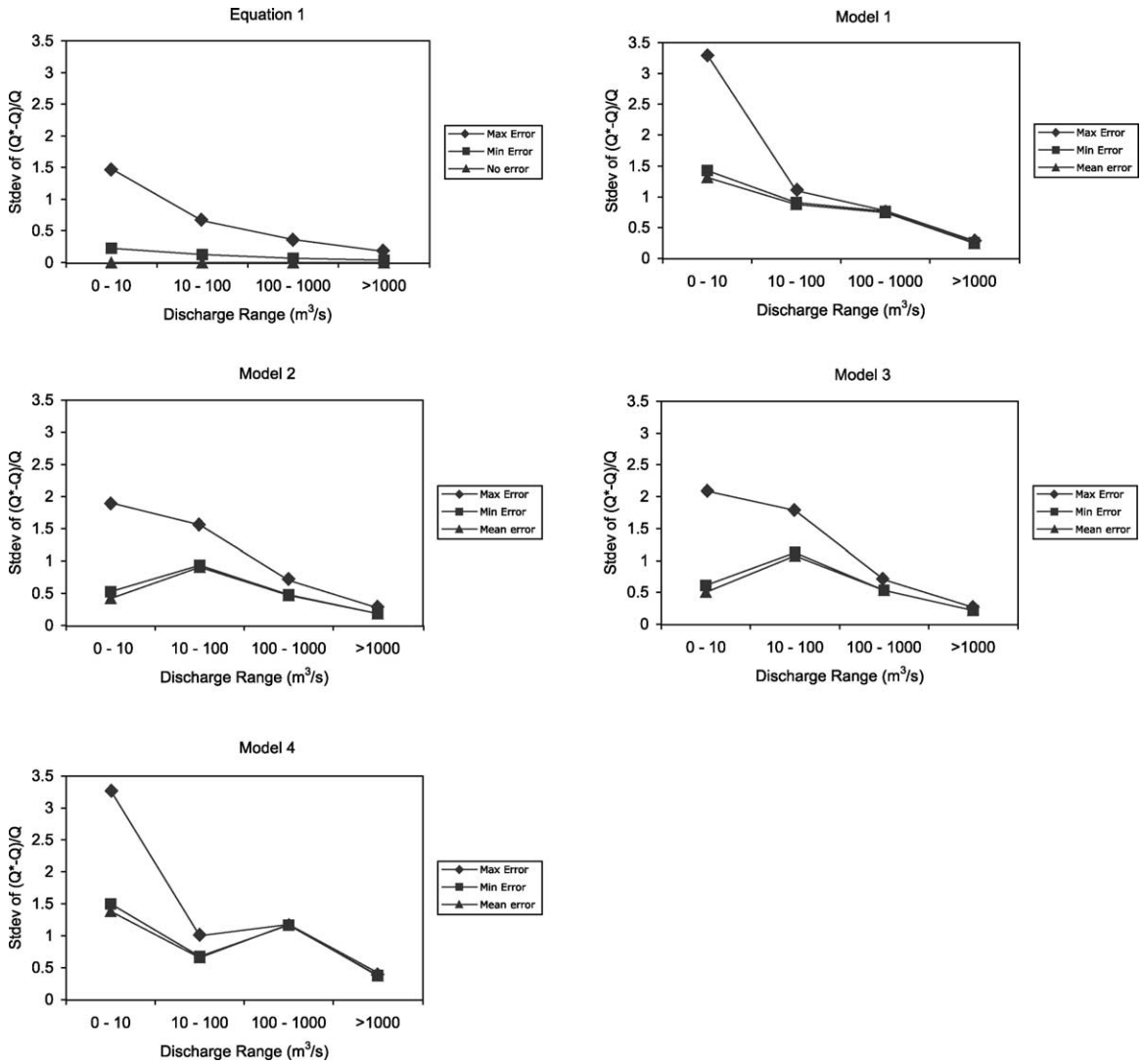

Fig. 4. Standard deviation of the relative residuals assuming high (maximum) and low (minimum) measurement error in the dynamic variables as compared to no (mean) assumed measurement error. The dynamic variables are width (W), average depth (Y) and average velocity (V). Ninety five percent of the assumed maximum errors are within ±10 m for W, ±0.5 m for Y and ±0.5 m/s for V. Ninety five percent of the assumed minimum errors are within ±1 m for W, ±0.1 m for Y and ±0.1 m/s for V.

Eq. (1), which includes uncertainty in all three dynamic variables, and indicates that uncertainty in V has a larger impact on prediction variability than does uncertainty in Y (comparing Model 1 and 2).

The impact of minimum uncertainty is not large within any discharge category, although as in the maximum uncertainty case it is most pronounced for discharge below 10 m^3/s. However, if the minimum measurement uncertainty is achieved for all dynamic variables, predicting discharge with Eq. (1) would result in a standard deviation in the relative residual (percent error) of less than 25% for discharges less than 10 m^3/s, less than 15% for discharge in the range 10–100 m^3/s and less than 10% for discharge greater than 100 m^3/s. The impact of minimum measurement uncertainty using Models 1, 2, 3 or 4 is less than 15% for discharge less than 10 m^3/s, and less than 10% for all other discharge categories. The plots in Fig. 3 show that if the minimum measurement uncertainty can be achieved, uncertainty in the estimated discharge using the statistically based models is well below the uncertainty associated with the model itself (no error case).

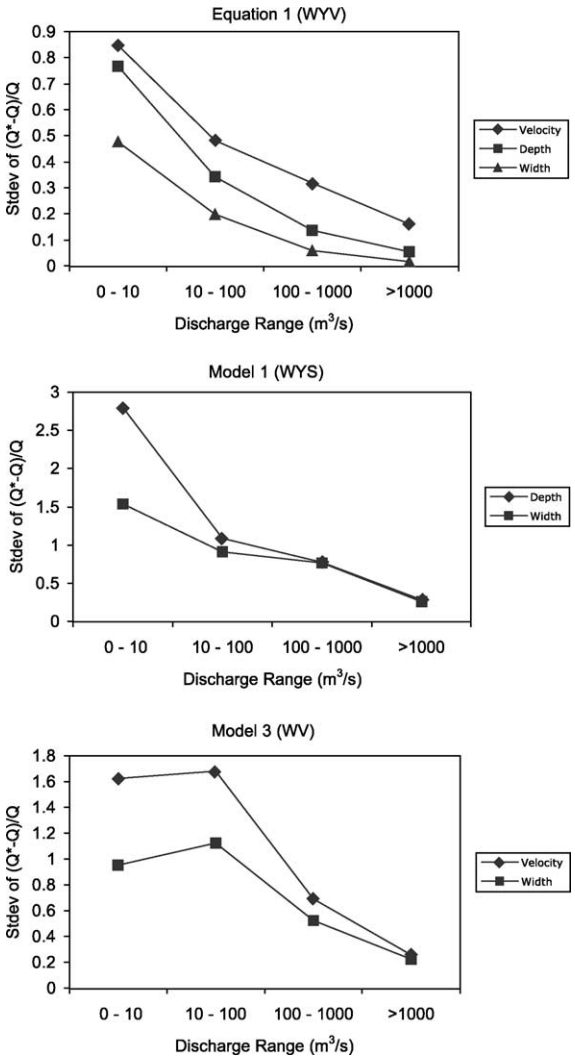

Fig. 5. Variation in the standard deviation of the relative residuals for prediction methods with more than one dynamic variable assuming error in only one variable at a time, showing the relative impact that error in the different dynamic variables has on prediction variability.

As suggested by comparing the plots for Model 1 and Models 2 and 3 in Fig. 4, there appears to be a different error response between Y and V. The differences in measurement uncertainty impact associated with the three dynamic variables were evaluated by introducing error into one variable at a time, and then comparing the standard devaition of the relative residuals. The results of this analysis are shown in Fig. 5 for Eq. (1), and Models 1 and 3. The plot for Eq. (1) shows that error in V has greater impact on the discharge estimate than does error in Y, and that error in W has the least impact. Comparing Models 1 and 3 shows that error in Y has the largest impact relative to W and V at low discharge (less than 10 m^3/s), and that error in V has a greater impact than error in Y for discharge greater than 10 m^3/s.

5. Discussion and conclusions

The advantage of a satellite based river discharge monitoring system is that it can fill in gaps where there is little or no information and obtain data over large areas simultaneously. Another advantage that satellite (or aerial) based measurement of hydraulic variables (particularly width) provides is the ability to observe variation over a reach, thus enabling a reach averaged value to be derived and minimizing the local variability that is specific to single cross-sections. Development of a general method to estimate river discharge using river channel hydraulic information observed from existing space or aerial platforms can be accomplished with statistical relationships developed from river data bases. If the water surface

velocity of a river can be observed with doppler lidar and used to estimate the average cross-sectional velocity and if the water-surface elevation can be used to estimate the average depth, all elements of Eq. (1) can be obtained remotely and the discharge in the river can be directly calculated.

The use of Eq. (1) is the preferred method to estimate discharge because it does not rely on a statistical derivation, shows the least overall prediction variance, and because it is applicable to any river under any flow conditions. However, it is likely that not all elements of Eq. (1) can be observed at the same time with confidence, thus statistically based models such as described by Models 1, 2, 3 and 4 can be used in these situations with reasonable accuracy, averaging $\pm 20\%$ or less, with accuracy within approximately $\pm 50\%$ 2/3 of the time. This level of accuracy compares favorably with estimates derived from extrapolation of ground-based ratings and slope-area measurements of discharge. Measurement error analysis indicates that with anticipated maximum uncertainty in the values of the observed variables, the variability of discharge estimates is increased substantially for discharges less than 100 m^3/s, however assuming, a reasonable minimum measurement uncertainty (0.1 m accuracy in depth, 1 m accuracy in width and 0.1 m/s) prediction error variability is only slightly increased over the no-error case.

Models that use width and surface-velocity only to estimate discharge (Model 3) can be used in situations where slope cannot be measured, or where anthropogenic control of slope violates the hydraulic assumptions inherent in Models 1 and 2, assuming surface velocity can be effectively measured. However, width-velocity models appear to have a bias trend across a wide range of discharge, indicating that these models would perform better if calibrated for specific ranges of discharge. Future studies should focus on further development and validation of statistical models designed to discriminate between potential threshold values of flow or size of rivers.

The predictive models described above are applicable to within-bank discharge only, because these models did not include over-bank flow in the data base used to develop and evaluate them. However, estimating over-bank discharge would require the same information, i.e. the width of flow, the average depth of flow and the average velocity of flow. Alsdorf et al. (2000) has shown the feasibility of using interferometric SAR to map the surface relief of an inundated region of the Amazon, thus demonstrating that mapping flow paths within a flooded area is possible. With this information, the discharge within the flooded area could be estimated and resolved in the downstream direction using floodplain topography and water surface elevation to estimate the flow depths across the inundated area. As shown by Brakenridge et al. (1998), Bates and DeRoo (2000) and Horritt (2000), this information could also be used in conjunction with a hydraulic model to estimate the downstream discharge within a flooded region. Brakenridge and Knox (1998) used satellite images obtained from ERS-1 coupled with topographic information to develop a three dimensional picture of the flooded area (inlcuding depth and areal extent) which were then used to track the flood wave and estimate flood discharge using the HEC-2 river hydraulic model.

The successful use of Eq. (1) and Models 2 and 3 will depend on the ability to measure surface velocity from space. To this end, development and verification of this technology will greatly enhance the potential ability to measure river discharge from space. Additionally, use of Eq. (1) and Models 1, 2, 3 and 4 all depend on the ability to translate surface measurements of stage and/or velocity into average values for the channel section under observation. Thus, techniques to estimate the average water depth in a channel section based on observation of water-surface elevation and techniques to estimate the average velocity in channel section based on measurements of surface velocity need to be developed and verified. Another issue of concern is that currently deployed altimeters cannot accurrately obtain water surface elevations on rivers less than several hundred meters wide. However, there is an indication that these same altimeters can observe much smaller rivers with similar accuracy by effecting a change in the on-board signal processing (Rodriquez, pers. commun., 2001). Also, laser altimeters may provide much greater accuracy with reduced observation size limitations relative to radar altimeters. The potential improvements in river stage measurement indicated by these developments need to be evaluated.

Elements of this research were funded by NASA grant numbers NAG5-7601 and NAG5-8683. We would like to acknowledge valuable review comments from G. Robert Brakenridge, Department of Geography, Dartmouth College, and William Kirby of the United States Geological Survey. In addition, we are indebted to Balazs Fekete, Research Scientist at the Institute for the Study of Earth, Oceans and Space at the University of New Hampshire for providing insight and ideas which contributed to much of this work.

References

Alsdorf, D.E., Melack, J.M., Dunne, T., Mertes, L.A.K., Hess, L.L., Smith, L.C., 2000. Interferometric radar measurements of water level changes on the Amazon River flood plain. Nature 404, 174–177.

Alsdorf, D.E., Smith, L.C., Melack, J.M., 2001. Amazon floodplain water level changes measured with interferometric SIR-C radar. IEEE Transactions on Geoscience and Remote Sensing 39 (2), 423–431.

Barnes, H.H., 1967. Roughness Characteristics of Natural Channels, USGS Water Supply Paper 1849, p. 213.

Barrett, E., 1998. Satellite remote sensing in hydrometry. In: Herschey, (Ed.), Hydrometry: Principles and Practices, Second ed., Wiley, Chichester, pp. 199–224.

Bates, P.D., DeRoo, A.P.J., 2000. A simple raster-based model for flood inundation simulation. Journal of Hydrology 236, 54–77.

Birkett, C.M., 1998. Contribution of the TOPEX NASA radar altimeter to the global monitoring of large rivers and wetlands. Water Resources Research 34 (5), 1223–1239.

Birkett, C.M., Mertes, L.A.K., Dunne, T., Costa, M.H., Jasinski, M.J., 2002. Surface Water Dynamics in the Amazon Basin: Application Of Satellite Radar Altimetry, presentation 2nd International LBA Scientific Conference, Manaus, Amazonas, Brazil July 7–10.

Brakenridge, G.R., Knox, J.C., Paylor, E.D., Magilligan, F.J., 1994. Radar remote sensing aids study of the Great Flood of 1993. EOS Trans., American Geophysical Union EOS Trans. 75 (45), 521–527.

Brakenridge, G.R., Tracy, B.T., Knox, J.C., 1998. Orbital SAR remote sensing of a river flood wave. Journal of Remote Sensing 19 (7), 1439–1445.

Bray, D.I., 1979. Estimating average velocity in gravel-bed rivers. Journal of the Hydraulic Division ASCE HY9, 1103–1123.

Chow, V.T., 1959. Open-Channel Hydraulics, McGraw-Hill, New York, p. 680.

Coon, W.F., 1998. Estimation of Roughness Coefficients for Natural Stream Channels with Vegetated Banks, US Geological Survey Water Supply Paper 2441, p. 133.

Costa, J.E., Spicer, K.R., Cheng, R.T., Haeni, F.P., Melcher, N.B., Thurman, E.M., 2000. Measuring stream discharge by non-contact methods: A proof-of-concept experiment. Geophysical Research Letters 27 (4), 553–556.

Davidian, J., 1984. Computation of Water Surface Profiles in Open Channels, US Geological Survey Techniques of Water-Resources Investigations. Book 3, Chapter A15, p. 47.

Dickerson, W.T., 1967. Accuracy of discharge determinations, Hydrology Papers, Colorado State University, Fort Collins Colorado, p. 20.

Dingman, S.L., Sharma, K.P., 1997. Statistical development and validation of discharge equations for natural channels. Journal of Hydrology 199, 13–35.

Dingman, S.L., 1984. Fluvial Hydrology, W.H. Freeman, New York, p. 383.

Dunne, T., Mertes, L.A.K., Meade, R.H., Richey, J.E., Forsberg, B.R., 1998. Exchanges of sediment between the floodplain and channel of the Amazon River in Brazil. GSA Bulletin 110 (4), 450–467.

Dury, G.H., 1976. Discharge prediction, present and former, from channel dimensions. Journal of Hydrology 30 (3), 219–245.

Emmitt, G.D., 2001. Personal communication. Simpson Weather Associates, Charlottesville, VA.

Fekete, B.M., Vorosmarty, C.J., Grabs, W., 1999. Global, composite runoff fields based on observed river discharge and simulated water balance, WMO-Global Runoff Data Center Report, 22., p. 114.

Herschey, R.W., 1998. Flow measurement. In: Herschey, (Ed.), Hydrometry: Principles and Practices, Second ed., Wiley, Chichester, pp. 9–83.

Hicks, D.M., Mason, P.D., 1991. Roughness Characteristics of New Zealand Rivers, New Zealand DSIR Marine and Freshwater Resources Survey, Wellington, NZ, p. 329.

Horritt, M.S., 2000. Calibration of a two-dimensional finite element flood flow model using satellite radar imagery. Water Resources Research 36 (11), 3279–3291.

Horritt, M.S., Mason, D.C., Luckman, A.J., 2001. Flood boundary delineations from synthetic aperture radar imagery using a statsitical active contour model. Journal of Remote Sensing 22 (13), 2489–2507.

IAHS Ad Hoc Committee, 2001, 2001. Global water data: a newly endangered species, EOS Transactions. American Geophysical Union 82 (5), 54see also 56, 58.

Jarrett, R.D., 1984. Hydraulic of high gradient streams. ASCE Journal of Hydraulic Engineering 110, 1519–1539.

Kirby, W.H., 1987. Linear error analysis of slope-area discharge determinations. Journal of Hydrology 100, 315–339.

Koblinsky, C.J., Clarke, R.T., Brenner, A.C., Frey, H., 1993. Measurement of river level with satellite altimetry. Water Resources Research 29 (6), 1839–1848.

Kuprianov, V.V., 1978. Aerial methods of measuring river flow. In: Herschey, (Ed.), Hydrometry: Principles and Practices, First ed., Wiley, Chichester, pp. 473–478.

M.J. Jasinski, C.M. Birkett, S. Chinn, M.H. Costa, (2001). Abstract, NASA/NOAA GAPP and Hydrology Principal Investigators Meeting, April 30-May, Potomac MD.

Leliavsky, S., 1966. An Introduction to Fluvial Hydraulics, Dover, New York.

Leopold, L.B., Wolman, M.G., Miller, J.P., 1964. Fluvial Processes in Geomorphology, W.H. Freeman, New York, p. 522.

Mertes, L.A.K., Dunne, T., Martinelli, L.A., 1996. Channel-floodplain geomorphology along the Solimes–Amazon River, Brazil. GSA Bulletin 108 (9), 1089–1107.

NASA Earth Observing System GLAS Science Team, 1997, 1997. Geoscience Laser Altimeter System (GLAS) Science Requirements, ICES-UTA-SPEC-001, GLAS-UTA-REQ-001.

Oltman, R.E., 1968. Reconnaissance investigations of the discharge and water quality of the Amazon River. US Geological Survey Circular 552, p. 16.

Osterkamp, W.R., Lane, L.J., Foster, G.R., 1983. An analytical treatment of channel-morphology relations. US Geological Survey Professional Paper 1288, p. 50.

Rantz, S.E., et al., 1982. Measurement and computation of streamflow. Measurement of Stage and Discharge, US Geological Survey Water Supply Paper, Vol. 1., p. 284.

Riggs, H.C., 1976. A simplified slope-area method for estimating flood discharges in natural channels. US Geological Survey Journal of Research 4, 285–291.

Rodriquez, E., 2001. Personal communication. NASA/Jet Propulsion Laboratory.

Rosgen, D.L., 1994. A Classification of Natural Rivers, Catena, 22, 169–199.

Sippel, S.J., Hamilton, S.K., Melack, J.M., Choudhury, B.J., 1994. Determination of inundation area in the Amazon River floodplain using SMMR 37 GHz polarization difference. Remote Sensing Environment 48, 70–76.

Smith, L.C., Isacks, B.L., Bloom, A.L., Murray, A.B., 1996. Estimation of discharge from three braided rivers using synthetic aperture radar satellite imagery. Water Resources Research 32 (7), 2021–2034.

Smith, L.C., 1997. Satellite remote sensing of river inundation area, stage, and discharge: a review. Hydrological Processes 11, 1427–1439.

University of Wisconsin Environmental Remote Sensing Center, 2001.

US Geological Survey, 2001. Streamflow measurement data base, http://water.usgs.gove/nwis/measurements

Vorosmarty, C., Birkett, C., Dingman, L., Lettenmaier, D.P., Kim, Y., Rodriguez, E., Emmit, G.D., Plant, W., Wood, E., 1999. NASA Post-2002 Land Surface Hydrology Mission Component for Surface Water Monitoring, HYDRA_SAT, A Report from the NASA Post 2002 LSHP Planning Workshop, Irvine CA April 12–14, p. 53.

Vorosmarty, C.J., Willlmott, C.J., Choudhury, B.J., Schloss, A.L., Stearns, T.K., Robeson, S.M., Dorman, T.J., 1996. Analyzing the discharge regime of a large tropical river through remote sensing, ground-based climatic data and modeling. Water Resources Research 32, 3137–3150.